Separation of Frequency Coexisting Vibration Signals in Wind Turbines Gearboxes

Javier E. Kolodziej, Gonzalo I. Vera Okulczyk, Sergio E. Moya, Fernando Botterón
Research and Development in Electronics Engineering Group (GID-IE)
Misiones Institute of Materials (IMAM)
National University of Misiones (UNaM) - National Scientific and Technical Research Council (CONICET)
Oberá, Argentine
koloj@fio.unam.edu.ar

***Abstract*— In this paper, a method for separation of vibration signals coexisting in the same frequency bin and coming from different mechanicals pieces is presented. A blind source separation method for vibration signals in gearboxes based on a clustering technique is applied. The proposed method uses the fact that spatial separation of vibration sources produces a difference in the hermitian angle between vectors composed by samples of the discrete Fourier transform of the signals measured and a reference vector. For simulations and a real case considering a wind turbine gearbox, time segments with signals providing from different mechanical pieces are identified.**

Keywords*— *frequency coexisting signals; gearbox; hermitian angle; vibration; wind turbine.

I. Introduction

Gearboxes are vital pieces in transmission mechanisms on rotating machines. Especially, in wind turbines they are essential to adjust the rotational speed of blades to the generator itself. Eolic generators can supply a large amount of power and critical failures may produce huge economic losses. Gearboxes are the largest contributor to turbine downtime and the costliest to repair [1]. That is the reason why faults detection in gearboxes has been studied for a long time, contributing to the development of applying condition monitoring and fault diagnosis (CMFD) technologies.

A large literature reports several technologies and applications for fault diagnostic in gearboxes. Since they are complex systems, multiple failures on the same or different elements can take place at the same time, namely hybrid faults [2]. Recently, an enormous effort has been focused on diagnose hybrid faults by using vibration signals, and the main strategy is try to decouple each fault signal, but still a particularly challenging situation, when fault signals providing from different components are narrowband and located in very similar frequency bands [3].

In this sense, a few methods could be applied in that particular situation using techniques such as empirical mode decomposition [4], time-frequency domain [5], morphological component analysis [6] order tracking, independent components analysis (ICA), and blind source separation (BSS) [7]. Meanwhile, aiming to reduce the influence of the position of only one sensor in the fault detection, a growing trend exists in the use of multiple sensors. That led to the need of a multivariable framework to analyze vibration signals. In this context, current options are mainly limit to variations of multivariate empirical mode decomposition (MEMD) [8] and BSS [2]. Mostly, methods based on BSS are preferred due the theoretical support. The aim of BSS is to distinguish among different signals from a combination of them without knowing the parameters of the combination model. Those algorithms usually are developed considering instantaneous combination or convolutive combination. However, in mechanical systems, mixtures of vibration signals most often are of the convolutive type [9]. A family of algorithms based on independent component analysis (ICA) are the most frequently used in BSS, and particularly in the separation of narrow band and located in the same frequency band signals [2]. However, ICA requires statistical independence between the source signals. In gearboxes vibration analysis, the vibration sources excited by the machine components can be statistically dependent.

In this work, we deal with the problem of decoupling vibration fault signals coexisting in the same frequency bin in gearboxes without the assumption of independence of the sources but only are sparse in the time-frequency domain and considering convolutive mixtures. Unlike [2] it is achieve decoupling of high correlated signals, but considering that are mixed in instantaneous mode.

This paper is organized as follow: Section II describes the signals propagation model considered. Section III explains the source identification in the frequency domain. Section IV applies the method in a simulated system. Section V performs in a real environment. Finally, conclusions are summarized in Section VI.[†]

[†] This work was supported by PIO UNaM-CONICET 2017 / 2018 237-201601-00001

II. SIGNALS COMBINATION MODEL IN TIME DOMAIN AND TIME-FREQUENCY DOMAIN

In this Section, the convolutive mixture signals model in the time domain and the equivalent model in the time-frequency domain considered in this work are presented.

The mathematical expression to model the convolutive combination of fault vibration signals can be expressed as

$$x_p(n) = \sum_{q=1}^{Q} h_{pq}(n) * s_q(n) = \sum_{l=0}^{L-1} h_{pq}(l) s_q(n-l) \text{ for } p = 1,..,P \quad (1)$$

where p is the sensor index, q is the fault source index, P is the number of sensors, Q is the number of sources, $h_{pq}(n)$ is the impulse response of the combinational filters modeling the propagation path from source q to sensor p, L is the combinational filter length (assuming FIR filters), $s_i(n)$ represents i-th source signal, and $x_i(n)$ the i-th sensor signal. Figure 1 presents a drawing of the signals propagation model considered in this paper.

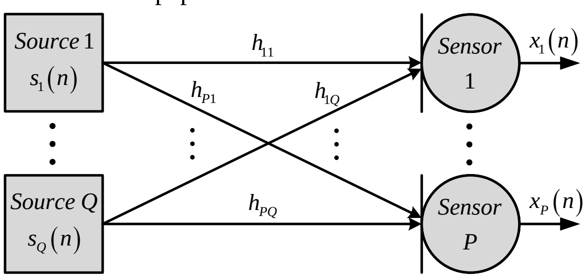

Figure 1. Signal propagation model from the fault sources to the sensors.

An extensively applied approach to deal with convolutive mixtures signals implies to represent them in the frequency domain [10]–[18]. Practical implementations require the use of short-time Fourier transform (STFT), which derives in a time-frequency domain combination model as [19]

$$\mathbf{X}(k,t) = \mathbf{H}(k)\mathbf{S}(k,t) = \sum_{q=1}^{Q} \mathbf{H}_q(k) S_q(k,t), \quad (2)$$

where $\mathbf{X}(k,t) = [X_1(k,t),... X_P(k,t)]^T$, is a column vector with the samples in the frequency bin k of the discrete Fourier transform (DFT) of a segment of $x_p(n)$ defined as

$$x_{p,t}(n) = \begin{cases} x_p(n+tN), & 0 \le n \le N-1 \\ 0, & \text{for others values of } n, \end{cases} \quad (3)$$

$\mathbf{S}(k,t) = [S_1(k,t),... S_Q(k,t)]^T$ is a column vector with the samples of the DFT of a segment of the source signals for the Q sources in the frequency bin k, $\mathbf{H}_q(k) = [H_{1,q}(k),... H_{P,q}(k)]^T$ is a column vector with the samples of the DFT in the frequency bin k of the impulse response of the combinational filters from source q to the P sensors. Finally, matrix $\mathbf{H}(k) = [\mathbf{H}_1(k) \; ... \; \mathbf{H}_Q(k)]^T$ groups the Q vectors $\mathbf{H}_q(k)$.

Note that t is used as block index and it is assumed that the impulse response of the combinational filters remains constant for all t.

III. FAULT SOURCE SEPARATION IN THE TIME-FEQUENCY DOMAIN

In this Section, the procedure to separate faults signals coexisting in the same frequency bin is presented. A fundamental assumption is that (2) is a disjoint representation of the source signals, which means that the signals are sparse in the TF domain. This condition was also assumed in [20] and can be supported in the amplitude modulation effect in vibration signals [21]. So, for a particular block, t_i, and frequency bin, k_j, $\mathbf{X}(k_j,t_i)$ is related with only one source $s_q(n)$ as

$$\mathbf{X}(k_j,t_i) = \mathbf{H}_q(k_j) S_q(k_j,t_i). \quad (4)$$

Considering that $\mathbf{H}_q(k_j)$ is a complex column vector, when it is multiplied by a complex scalar $S_q(k_j,t_i)$, as in (4), their values and angles change [22]. However, it could be verified that the hermitian angle between $\mathbf{H}_q(k_j)$ and a reference vector $\mathbf{r}$ would be equal to the hermitian angle between $\mathbf{X}(k_j,t_i)$ and the same reference vector $\mathbf{r}$ during the time when only the source $s_q(n)$ is present and probably it would change when another source predominates [23]. So, the hermitian angle can be used to classify signal segments considering the source. Due the noise, the hermitian angles related with a determined source are not constant, so it is necessary to use a clustering method to group together angles that can be considered that are related with the same source.

The use of hermitian angles to separate signals was initially proposed in [23] considering speech signals. In [20], a similar procedure is applied to gearboxes fault signals, combined with the variational mode decomposition, but focused into separate the stationary and no stationary components of wide band signals, similarly to [9] where STFT is applied with this end. In this work, we limit the analysis to only one target bin, where, on account of a previous knowledge of the system, more than one stationary fault signal could coexist.

In the following, the algorithm proposed to separate the signals is summarized:

(i) To define a reference vector with non-zero components. An example for the case of two sensors is $\mathbf{r} = [1+j1, 1+j1]^T$.

(ii) To compute the hermitian angle between $\mathbf{X}(k,t)$ and $\mathbf{r}$, for the target bin k and all t, as [24]:

$$\theta_H(k,t) = \arccos\left(\left| \frac{\mathbf{X}^H(k,t)\mathbf{r}}{\|\mathbf{X}(k,t)\| \|\mathbf{r}\|} \right| \right) \quad (5)$$

This step is similar to the proposed in [23].

(iii) To use k-means clustering algorithm to group $\theta_H(k,t)$ in Q groups in the frequency bin k.

(iv) To define binary masks to indicate if the segment belongs or not to each group.

IV. Application to Gearbox Vibrations Signals: Simulation Results

In the following, it is shown how the proposed method can be used to individualize signals within the same frequency band and coming from different pieces in a gearbox.

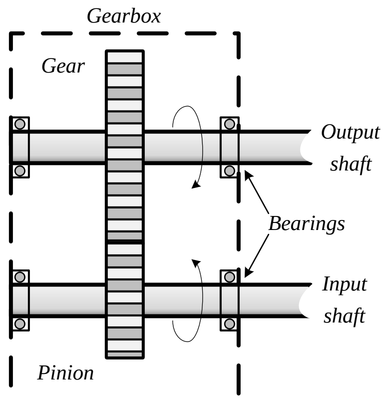

Figure 2. Simulated gearbox.

A. Considered problem

It is considered the gearbox represented in Figure 2, that consist of a 9-tooth pinion, $N_p = 9$, meshing with a 32-tooth gear, $N_g = 32$. The pinion is coupled to an input shaft connected to a prime mover. The gear is connected to an output shaft. The shafts are supported by roller bearings on the gearbox housing. Two accelerometers, A_1 and A_2 are placed on the bearing and gearbox housings, respectively. The pinion rotates at a rate $f_p = 22.5$ Hz or 1,350 rpm. The rotation speed of the gear and the output shaft is

$$f_g = f_p \times \frac{N_p}{N_g} = 6.33 \text{ Hz}. \tag{6}$$

The tooth-mesh frequency, the rate at which gear and pinion teeth periodically engage, is:

$$f_M = f_P \times N_P = f_G \times N_G = 202.5 \text{ Hz}. \tag{7}$$

For better resolution in spectral analysis, the sample frequency to the accelerometers signals is selected as a multiple of f_M, so $f_s = 20,250$ Hz is considered.

B. Considered faults

In this example, three types of faults in the gearbox are considered, according shown in Fig.3:

- Local fault on a gear tooth: assume that the gear is suffering from a local fault such as a spall. This results in a high-frequency impact occurring once per rotation [25]. In this example, it is arbitrarily assumed that the impact causes a 2 KHz vibration signal and occurs over a duration of about 8% of $1/f_M$. The impact repeats once per rotation of the gear.
- Eccentricity or pinion misalignment: it is a distributed fault, causing higher-level sidebands that are narrowly grouped around integer multiples of the mesh frequency [26]. In this example, three sidebands are considered.
- Rolling element bearing fault: Assume that the bearing supporting the pinion shaft is affected by a localized fault in the inner race. Faults in bearings have characteristic frequency, for the case considered here, it is [27]

$$f_{BPI} = \frac{\eta \times f_{Gear}}{2}\left(1 + \frac{\delta}{\rho}\cos\theta\right) = 202.5 \text{ Hz}, \tag{8}$$

where η is the number of rolling bearings, δ is the diameter of rolling elements, θ is the contact angle, and ρ is the pitch diameter of the bearing. Table 1 presents the values of these parameters.

From (7) and (8) can be conclude that f_{BPI} and f_M are coincident, so in this band we focus our analysis and, as we have to separate two vibration signals, are selected two clusters for the k-means algorithm.

Table 1. Bearing parameters

Parameters	η	δ	ρ	θ
Values	61	0.0118	0.23	16.5443

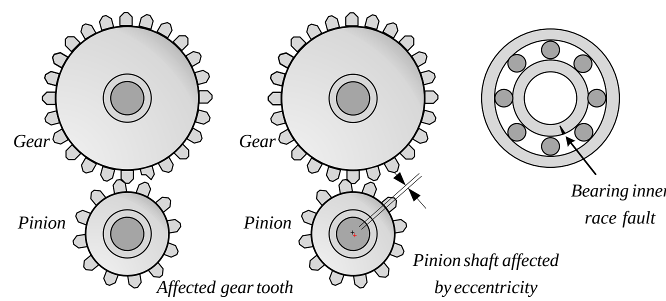

Figure 3. Considered faults: (a) Fault on a gear tooth. (b) Pinion misalignment. (c) Rolling element bearing fault.

C. Simulation Results

In this example, are considered two signal sources: one containing the bearing fault signal, $s_1(n)$, and the other containing the gear teeth fault and pinion misalignment, $s_2(n)$. Both signals, $s_1(n)$ and $s_2(n)$, propagate considering four different paths: $h_{11}(n)$, $h_{12}(n)$, $h_{21}(n)$, and $h_{22}(n)$, according is shown in Fig. 1, resulting in the signals measured through the accelerometers, $x_i(n)$. The signal sources and the combined signals are shown in Figure 4. The impulse responses considered for each propagation path are shown in Figure 5.

Applying the procedure detailed in Section III, with blocks of 200 samples ($N = 200$) and focusing on the frequency bin associated to 202.5 Hz, the values of hermitian angle for each block during 20 seconds (approximately 2000 blocks) are obtained. Then, the k-means algorithm is applied to separate the hermitian angles in two groups. The obtained results are shown in Figure 6 and Fig. 7. From these results, it is possible to consider that in time segments associated with one hermitian angle group, one of the fault vibration signal source is the most relevant. For the segments associated to the other hermitian angle group, another source will be more relevant.

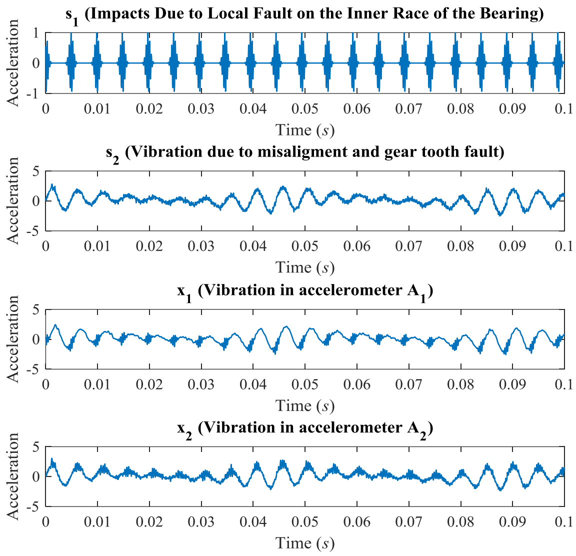

Figure 4. Fault source signals and sensing signals. (a) Bearing fault. (b) Gear faults. (c) Signal at sensor A_1. (d) Signal at sensor A_2.

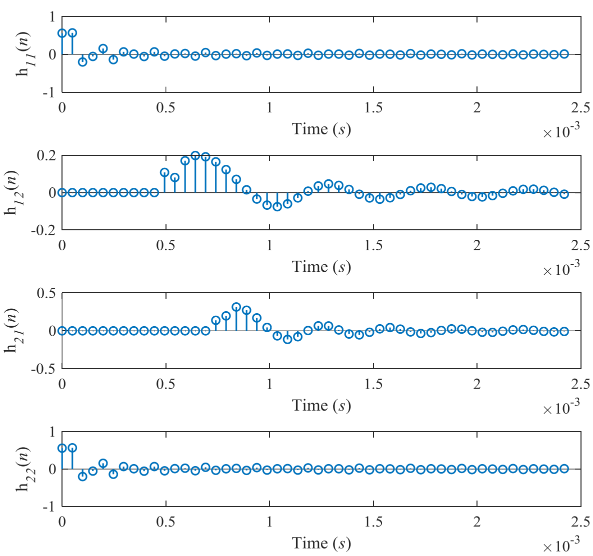

Figure 5. Impulse responses for propagation paths.

Using this reasoning, the accelerometers signals can be separated in two groups according is illustrated in Figure 8 (note the coherence with Fig. 7)

Finally, the temporal characteristics of the fault signals can be used to verify the separation correctness in this particular example, comparing the signals of Figure 4 and Figure 8. Can be effectively observed that when the gear signals decrease and the bearing signal become the most relevant it is recognized one group. For other hand, when the gear vibration signals increase, it is identified the other group. So, it is possible to isolate bearing fault signals. Note that the proposed method can individualize fault signals without considering the signal amplitude and in a blind way.

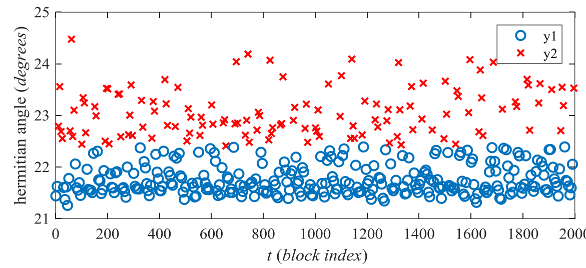

Figure 6. Hermitian angles for the 202.5 Hz frequency bin.

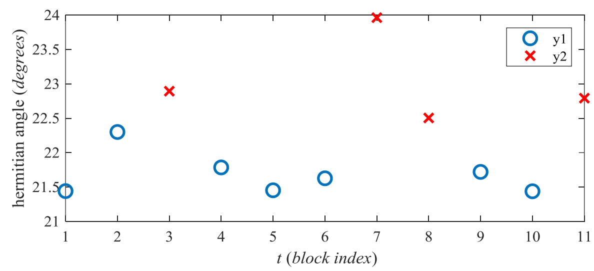

Figure 7. Zoom of hermitian angles at the time period showed below.

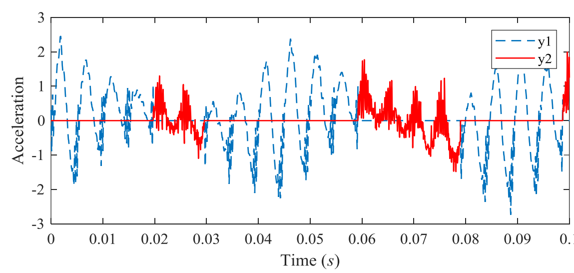

Figure 8. Accelerometer A1's signal. Signal where prevails bearing fault (blue dashed line). Signal where prevails gear vibration (red solid line).

V. Application to Gearbox Vibrations Signals: Real Case

In this section the results obtained applying the proposed method for a real situation are presented. A data set provided by the National Renewable Energy Laboratory for a wind turbine drive train is considered. Data correspond to an upwind turbine, with a rated power of 750kW. The turbine generator operates at 1800 rpm and 1200 rpm nominal. It is composed of one low speed (LS) planetary stage and two parallel stages, as shown in the expanded view in Fig. 9. The analysis is concentrated in the inner race fault signal for bearing D (called ISS-A in Fig. 9), $f_{BI} = 72.9\,\text{Hz}$ and the second harmonic of the planet gear mesh between the ring and the planet, $f_{M2nd} = 73.71\,\text{Hz}$. The proximity of frequencies become very difficult to draw a conclusion about the state of bearing D with a spectral analysis [27], such it is shown in Fig. 10. In this figure data from two conditions, healthy and damaged, considering three accelerometers (Table 2), are compared. An increment in the peak related with 73Hz can be observed, however, it is not sufficient to conclude that this effect is due exclusively to a fault in the bearing D [27].

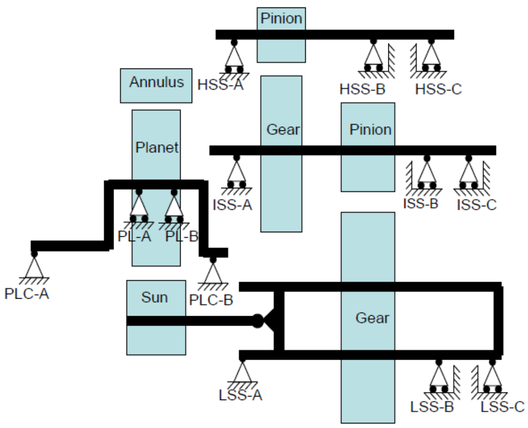

Figure 9. Considered Gearbox.

Table 2. Accelerometers descriptions

Sensor Label	Description
AN4	Ring gear radial 12 o'clock
AN6	ISS radial
AN7	HSS radial

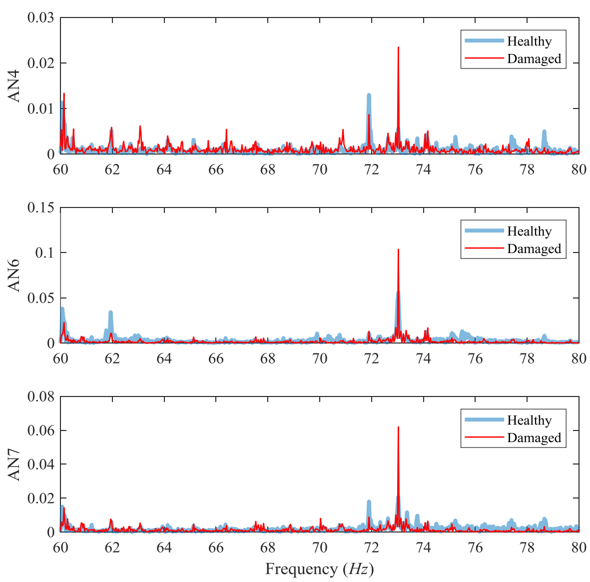

Figure 10. Spectral analysis. (thick blue line) Healthy case. (slim red line) Damaged case.

Appling the proposed method to the same data, considering blocks of 1100 samples ($N = 1100$) and the frequency bin associated to 73 Hz, the values of hermitian angle for each block are obtained for the healthy and damaged conditions. The resulting hermitian angles are presented in Fig. 11.

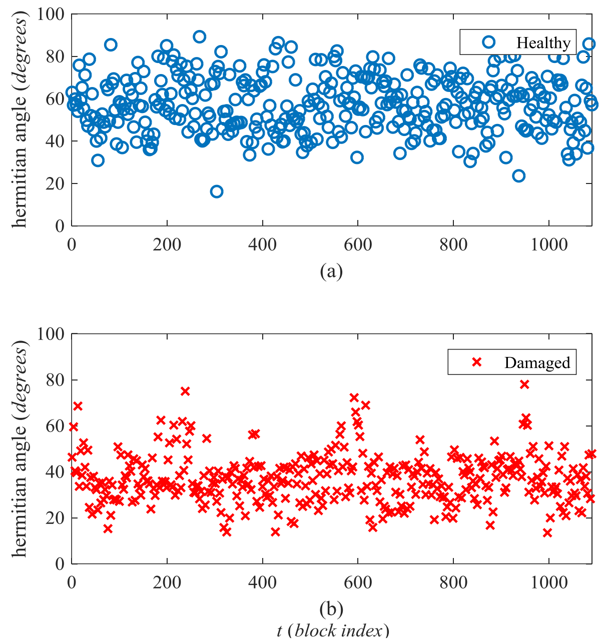

Figure 11. Heamitian angles for 73Hz frequency bin. (a) Healthy case. (b) Damaged case.

As seen in Fig. 11(a), in the healthy case, the angles are uniform and concentrated, without polarizations, which can suggest that only one source exist. On the other hand, the damaged case associated with Fig. 11(b) presents a polarization in the hermitian angles according the time proceeds, so, can be inferred that two fault sources are involved. Then, k-means is applied to group the angles of the damaged case in two clusters, related to each source, as it is shown in Figure 12 and Fig. 13. Finally, the clusters separation is used to relate signal segments to the inner race fault signal or the second harmonic of the planet gear mesh between the ring and the planet as is illustrated in Fig. 14.

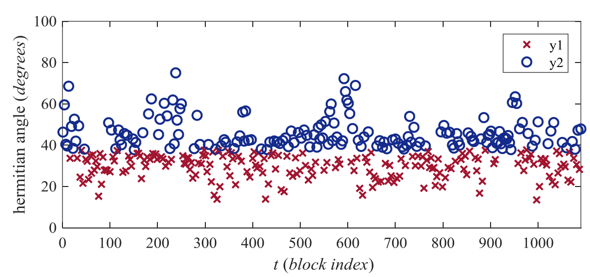

Figure 12. Clustering hermitian angles for the damaged case at the time period showed below. (x) Cluster 1. (o) Cluster 2.

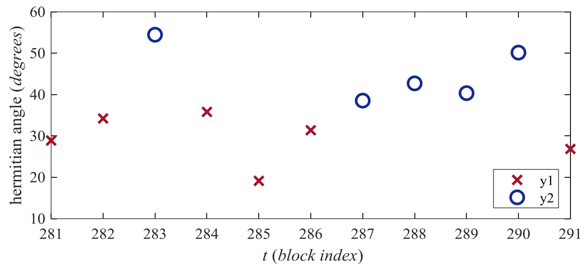

Figure 13. Zoom of hermitian angles for the damaged case. (x) Cluster 1. (o) Cluster 2.

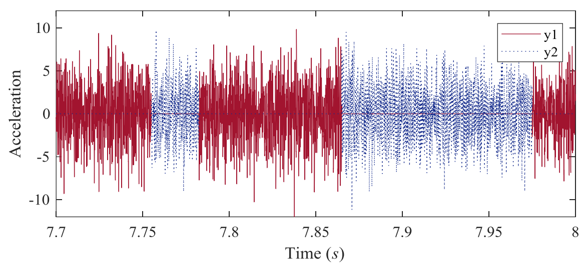

Figure 14. Signal separation according to the fault source prevalence.

Acknowledgment

Authors thank the US Department of Energy (DOE)/National Renewable Energy Laboratory (NREL) for providing the datasets to support this work, and, specially, to Dr. Shuangwen Sheng for the valuable recommendations. The authors also acknowledge the reviewers for their careful work

References

[1] S. Sheng, "Gearbox Typical Failure Modes, Detection and Mitigation Methods," *AWEA Operations & Maintenance and Safety Seminar*, vol. National Renewable Energy Laboratory/National Wind Technology Center, p. 24, Jan. 2014.

[2] Z. Li, Y. Jiang, C. Hu, and Z. Peng, "Recent progress on decoupling diagnosis of hybrid failures in gear transmission systems using vibration sensor signal: A review," *Measurement*, vol. 90, pp. 4–19, Aug. 2016.

[3] H. Luo, C. Hatch, M. Kalb, J. Hanna, and A. Weiss, "Analysis algorithms and diagnostics results from General Electric," *Wind turbine gearbox condition monitoring round robin study - vibration analysis*, vol. S. Sheng, National Renewable Energy Laboratory, Jul. 2012.

[4] Y. Lei, J. Lin, Z. He, and M. J. Zuo, "A review on empirical mode decomposition in fault diagnosis of rotating machinery," *Mechanical Systems and Signal Processing*, vol. 35, no. 1, pp. 108–126, Feb. 2013.

[5] L. S. Dhamande and M. B. Chaudhari, "Compound gear-bearing fault feature extraction using statistical features based on time-frequency method," *Measurement*, vol. 125, pp. 63–77, Sep. 2018.

[6] D. Yu, M. Wang, and X. Cheng, "A method for the compound fault diagnosis of gearboxes based on morphological component analysis," *Measurement*, vol. 91, pp. 519–531, Sep. 2016.

[7] T. D. Popescu, "Blind separation of vibration signals and source change detection – Application to machine monitoring," *Applied Mathematical Modelling*, vol. 34, no. 11, pp. 3408–3421, Nov. 2010.

[8] N. Rehman and D. P. Mandic, "Multivariate empirical mode decomposition," *Proceedings of the Royal Society of London A: Mathematical, Physical and Engineering Sciences*, vol. 466, no. 2117, pp. 1291–1302, May 2010.

[9] J. Antoni, "Blind separation of vibration components: Principles and demonstrations," *Mechanical Systems and Signal Processing*, vol. 19, no. 6, pp. 1166–1180, Nov. 2005.

[10] P. Smaragdis, "Blind separation of convolved mixtures in the frequency domain," *Neurocomputing*, vol. 22, no. 1, pp. 21–34, Nov. 1998.

[11] L. Parra and C. Spence, "Convolutive blind separation of non-stationary sources," *IEEE Transactions on Speech and Audio Processing*, vol. 8, no. 3, pp. 320–327, May 2000.

[12] J. Anemüller and B. Kollmeier, "Amplitude Modulation Decorrelation For Convolutive Blind Source Separation," in *Proc Int Conf on Independent Component Analysis and Blind Source Separation*, 2000, pp. 215–220.

[13] N. Murata, S. Ikeda, and A. Ziehe, "An approach to blind source separation based on temporal structure of speech signals," *Neurocomputing*, vol. 41, no. 1, pp. 1–24, Oct. 2001.

[14] H. Sawada, R. Mukai, S. Araki, and S. Makino, "A robust and precise method for solving the permutation problem of frequency-domain blind source separation," *IEEE Transactions on Speech and Audio Processing*, vol. 12, no. 5, pp. 530–538, Sep. 2004.

[15] H. Saruwatari, S. Kurita, K. Takeda, F. Itakura, T. Nishikawa, and K. Shikano, "Blind Source Separation Combining Independent Component Analysis and Beamforming," *EURASIP J. Adv. Signal Process.*, vol. 2003, no. 11, p. 569270, Dec. 2003.

[16] R. Mukai, H. Sawada, S. Araki, and S. Makino, "Frequency domain blind source separation using small and large spacing sensor pairs," in *2004 IEEE International Symposium on Circuits and Systems (IEEE Cat. No.04CH37512)*, 2004, vol. 5, pp. V-1-V-4 Vol.5.

[17] A. Hiroe, "Solution of Permutation Problem in Frequency Domain ICA, Using Multivariate Probability Density Functions," in *Independent Component Analysis and Blind Signal Separation*, 2006, pp. 601–608.

[18] T. Kim, H. T. Attias, S. Y. Lee, and T. W. Lee, "Blind Source Separation Exploiting Higher-Order Frequency Dependencies," *IEEE Transactions on Audio, Speech, and Language Processing*, vol. 15, no. 1, pp. 70–79, Jan. 2007.

[19] H. Sawada, S. Araki, and S. Makino, "A Two-Stage Frequency-Domain Blind Source Separation Method for Underdetermined Convolutive Mixtures," in *2007 IEEE Workshop on Applications of Signal Processing to Audio and Acoustics*, 2007, pp. 139–142.

[20] Z. Li, Y. Jiang, Q. Guo, C. Hu, and Z. Peng, "Multi-dimensional variational mode decomposition for bearing-crack detection in wind turbines with large driving-speed variations," *Renewable Energy*, vol. 116, pp. 55–73, Feb. 2018.

[21] R. B. Randall and J. Antoni, "Rolling element bearing diagnostics—A tutorial," *Mechanical Systems and Signal Processing*, vol. 25, no. 2, pp. 485–520, Feb. 2011.

[22] J. H. Kwak and S. Hong, *Linear Algebra*, 2nd ed. Birkhäuser Basel, 2004.

[23] V. G. Reju, S. N. Koh, and I. Y. Soon, "Underdetermined Convolutive Blind Source Separation via Time-Frequency Masking," *IEEE Transactions on Audio, Speech, and Language Processing*, vol. 18, no. 1, pp. 101–116, Jan. 2010.

[24] K. Scharnhorst, "Angles in Complex Vector Spaces," *Acta Applicandae Mathematicae*, vol. 69, no. 1, pp. 95–103, 2001.

[25] MathWorks, "Rolling Element Bearing Fault Diagnosis - MATLAB & Simulink." [Online]. Available: https://la.mathworks.com/help/predmaint/examples/Rolling-Element-Bearing-Fault-Diagnosis.html. [Accessed: 12-Sep-2018].

[26] C. Scheffer and P. Girdhar, *Practical Machinery Vibration Analysis and Predictive Maintenance*. Elsevier, 2004.

[27] R. B. Randall, *Vibration-Based Condition Monitoring: Industrial, Aerospace and Automotive Applications*. 2010.